IEEE Access
Multidisciplinary | Rapid Review | Open Access Journal

Received 15 August 2023, accepted 19 October 2023, date of publication 25 October 2023, date of current version 2 November 2023.

Digital Object Identifier 10.1109/ACCESS.2023.3327337

RESEARCH ARTICLE

Identification of Single-Phase Line Break Fault Direction Based on Local Voltage Information in Small Current Grounding System Considering the Impact of DG

FAN YANG[1], HE LI[2], WEI HU[1], YANG LEI[1], HECHONG CHEN[1], AND YONGDUAN XUE[2], (Member, IEEE)

[1]Electric Power Research Institute, State Grid Hubei Electric Power Company, Wuhan 430077, China
[2]College of New Energy, China University of Petroleum (East China), Qingdao 266580, China

Corresponding author: He Li (l853664879@163.com)

This work was supported by the Project of State Grid Hubei Electric Power Company Ltd., under Grant 52153222001F.

ABSTRACT Line break faults commonly occur in distribution networks and pose the risk of electric shocks to nearby individuals and animals. This study aims to address the challenge of identifying the direction of a line break fault. Specifically, we develop a model for a single-phase line break fault in a small current grounding system and focus on analyzing the steady-state voltage changes on both sides of the fault point. The voltage characteristics of the ungrounded system and the resonant grounding system are compared and summarized. Based on these characteristics, a more reliable method is proposed to identify the single-phase line break fault direction by utilizing two types of local voltage information: the magnitude of the line-to-line voltage and the sequence of phase-to-earth voltage. Additionally, we analyze the effects of V/V wired potential transformer (PT) and distributed generation (DG). The proposed method can accommodate the high utilization rate of V/V wired PT in distribution networks and its practicality is unaffected by the connection of DG to the distribution network. The above analysis is verified through simulations. The findings of this study demonstrate that the direction of a single-phase line break fault can be reliably detected using local voltage information and can be further localized with the assistance of communication, thereby improving the level of relay protection in distribution networks.

INDEX TERMS Distribution network, small current grounding system, single-phase line break fault, steady-state voltage, fault direction, distributed generation.

I. INTRODUCTION

Small current grounding operations, including ungrounded systems and resonant grounding systems, are widely accepted in medium voltage distribution systems [1], [2], [3], [4], [5]. Due to external forces, loose connections, blown fuses, defective contact of circuit breaks, and meteorological disasters (thunderstorms, snow, strong gusts of wind), line break fault occurs frequently [6], [7]. According to references [8], [9], approximately 12% of the faults in 10kV distribution networks are line break faults. In recent years, the rapid transition from uncovered overhead lines to insulated overhead lines has increased the frequency of line break faults [10], [11]. Once the flashover develops into an electric arc on insulated lines, the electric arc cannot swing as how it is driven by electric force or wind on uncovered overhead lines. Eventually, consistent arcing at the fixed point will lead to a line break fault.

Line break faults can have a detrimental impact on various types of loads, particularly constant power loads. reference [7] introduced a control strategy to mitigate the effects of fault on loads, but it cannot eliminate line break faults.

The associate editor coordinating the review of this manuscript and approving it for publication was Mehrdad Saif.

The long-term existence of line break faults can also increase the risk of fires and even personal electrocution accidents, seriously threatening the safety and stability of the distribution network [12]. Nonetheless, line break faults typically result in very low fault currents, which makes their detection using existing conventional protective relaying schemes highly challenging [13]. Since single-phase line break faults are the most likely type of line break faults to occur, it is necessary to analyze the characteristics of single-phase line break faults and propose associated immediate detection approaches.

There are four types of single-phase line break faults: single-phase line break without earthing, single-phase line break with earthing at the system side, single-phase line break with earthing at the load side, and single-phase line break with earthing at both sides [14]. According to reference [15], a single-phase line break with earthing at both sides has the same fault characteristics as a single-phase-to-earth fault. Therefore, it can be resolved using traditional small current grounding fault diagnosis methods [16], [17], [18], [19], and the corresponding analysis is not duplicated in this paper.

Reference [20] conducted an analysis on the overvoltage characteristics of single-phase line break fault without earthing in resonant grounding systems. The study demonstrated that the fault can lead to overvoltages which may endanger the insulation of the network. However, reference [20] did not consider single-phase line break faults with earthing. In practical distribution networks, pure line break faults often escalate into line break faults with earthing when the broken conductors make contact with the ground. Our previous works [21], [22], respectively, investigated the voltage change characteristics on both sides of the fault point for different types of single-phase line break faults in ungrounded and resonant grounding systems. Nevertheless, a comprehensive summary of these characteristics is currently lacking, and no novel detection method has been proposed in either reference.

Reference [23] conducted a comparative analysis between measured phase currents and predicted phase currents to identify line break faults in effectively grounded distribution networks. The predicted phase currents were calculated using Residual Current Multiplying Factors. In reference [24], the detection of single-phase line break faults was based on the analysis of three-phase currents, with three-phase voltages used as an additional criterion to determine the presence of a ground fault. Reference [12] proposed a method that utilized voltage amplitude and phase on the low voltage side of the distribution transformer to differentiate line break faults from short-circuit faults. In reference [15], a line break fault detection method was introduced based on the differential principle of zero sequence voltage amplitude. This method required voltage information on both sides of the fault point and relied on communication. Lastly, reference [25] presented a deep learning identification method for single-phase line break faults, which combined variation mode decomposition and stacked auto encoder with double optimization.

Due to differences in neutral point grounding operations, certain proposed approaches cannot be directly applied to small current grounding systems. Furthermore, the references mentioned above, which utilize current characteristics as the criterion, are often limited by unbalanced loads and light load conditions. These constraints make conventional phase current and negative sequence current elements almost ineffective in detecting line break faults. Although the method proposed by reference [23] addresses the effects of unbalanced loads, it may still lose efficacy under light load conditions. Most of the aforementioned methods rely solely on single fault information to detect line break faults, which makes them less reliable compared to approaches that consider two or more fault information. The method proposed by reference [15] relies on communication and has high requirements on distribution network equipment. Furthermore, fault detection methods using depth learning models or intelligent algorithms have fewer practical applications, and their practicality remains uncertain.

In recent years, there has been a significant increase in the connection of distributed generations (DGs) to the distribution network, which can have an impact on the characteristics of line break faults [26]. Also, it should be noted that small current grounding operations are commonly used in suburban and rural areas. Due to limited investment in these areas, cost-effective V/V wired potential transformers (PTs) are often utilized for measuring devices [27]. However, V/V wired PTs are incapable of measuring phase-to-earth voltage. Therefore, existing fault detection methods that rely on phase-to-earth voltage information are not applicable in such situations, reducing their practicality.

In summary, there exists a deficiency in the analysis and summarization of the voltage characteristics of line break faults in small current grounding systems, and the existing line break fault detection methods have their own limitations. Therefore, it is necessary to summarize the characteristics of single-phase line break faults and propose a fault detection method that is simple, reliable, and practical. This paper makes the following contributions:

1) The characteristics of phase-to-earth voltages and line-to-line voltages on both sides of the fault point are analyzed. Additionally, the magnitude and phase range of phase-to-earth voltages are derived. Finally, a systematic comparison and summary are provided to highlight the fault voltage characteristics between the ungrounded system and the resonant grounding system.
2) Based on these characteristics, a more reliable method is proposed to identify the fault direction by utilizing two types of local voltage information: the magnitude of the line-to-line voltage and the sequence of phase-to-earth voltage. Furthermore, the practicality of the method is examined by investigating the impacts of V/V wired PT and DG.

The rest of this paper is organized as follows. Section II analyzes the voltage characteristics of single-phase line break

faults under different situations. Section III proposes a fault direction identification method and analyzes the effects of V/V wired PT and DG. Section IV introduces the fault location and processing method. Section V presents the case study results. Finally, Section VI concludes this paper.

II. VOLTAGE CHARACTERISTICS FOR SINGLE-PHASE LINE BREAK FAULT IN SMALL CURRENT GROUNDING SYSTEM

A. MODEL OF A SINGLE-PHASE LINE BREAK FAULT IN SMALL CURRENT GROUNDING SYSTEM

The single-phase line break fault in a small current grounding system can be modeled as shown in Fig. 1. Take the line break fault at phase A as an example. In Fig. 1, L and R_L represent the equivalent parallel inductance and resistance of the Petersen coil, respectively; $\dot{E}_A$, $\dot{E}_B$, $\dot{E}_C$ and $\dot{U}_A$, $\dot{U}_B$, $\dot{U}_C$ represent the phase-to-neutral voltages of the voltage source and phase-to-earth voltages of the three buses, respectively; L_1 and L_2 represent the equivalent circuits for all healthy feeders and the faulty feeder, respectively; N indicates the neutral point; O indicates the ground potential; $\dot{U}_{NO}$ represents the neutral voltage; A and A' represent the nodes on both sides of the fault point; C_1 and C_2 represent the capacitance-to-earth of each phase for all healthy feeders and the faulty feeder, respectively; x is the ratio of capacitance-to-earth downstream of the fault point to the total capacitance-to-earth of the faulty feeder, which represents the location of the fault point; R_d and R'_d represent the earthing resistance on both sides of the fault point; load impedances of three phases with a Y-connection are assumed to be balanced. Z_1 and Z_2 represent the load impedance in L_1 and L_2, respectively; compared to the capacitive reactance of the distribution line to the ground, the impedance of the distribution line is extremely small and can be neglected [28].

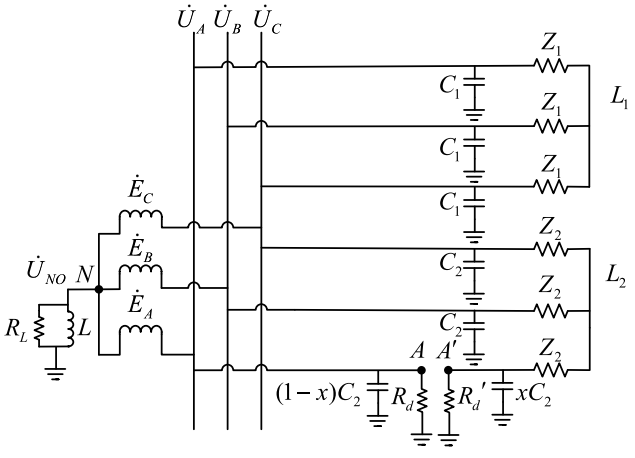

FIGURE 1. Diagram of a single-phase line break fault in a small current grounding system.

B. MATHEMATICAL EXPRESSION OF VOLTAGE ON BOTH SIDES OF THE FAULT POINT

According to Kirchhoff's Current Law, the $\dot{U}_{NO}$ for different types of single-phase line break faults can be written as follows:

Single-phase line break fault without earthing ($R_d = R'_d = \infty$):

$$\dot{U}_{NO} = \frac{x}{2k\,(v - jd)}\dot{E}_A \tag{1}$$

where v and d represent the detuning factor and damping ratio, respectively; k is the ratio of total system capacitance-to-earth to the faulty feeder's capacitance-to-earth; x/k represents the ratio of capacitance-to-earth downstream of the fault point to the total system capacitance-to-earth. The mathematical expressions for these factors can be written as:

$$\begin{cases} v = 1 - \dfrac{1}{3k\omega^2 C_2 L} \\ d = \dfrac{1}{3k\omega C_2 R_L} \\ k = \dfrac{C_1 + C_2}{C_2} \end{cases} \tag{2}$$

In ungrounded system, $v = 1$, $d = 0$.

Single-phase line break fault with earthing at the system side ($R'_d = \infty$):

$$\dot{U}_{NO} = \frac{3 - \left(3Z_2 + \frac{2}{j\omega x C_2}\right)\Big/ R_d}{\left(3Z_2 + \frac{2}{j\omega x C_2}\right)\Big/ R_d + \frac{6k}{x}(v - jd)}\dot{E}_A \tag{3}$$

Single-phase line break fault with earthing at the load side ($R_d = \infty$):

$$\dot{U}_{NO} = \frac{j\omega x C_2\,(3Z_2 f + 2) + f}{\left(3j\omega x C_2 Z_2 + \frac{3Z_2}{R'_d} + 2\right)\left[\frac{1}{R'_d} + 3k\omega C_2\,(d + jv)\right] - 3Z_2 f^2}\dot{E}_A \tag{4}$$

where $f = \mathrm{j}\omega x C_2 + 1/R'_{\mathrm{d}}$.

According to Fig. 1, the phase-to-earth voltage of A' can be written as:

$$\dot{U}_{A'} = \frac{-\frac{1}{2}\dot{E}_A + \dot{U}_{NO}}{1 + \frac{3Z_2}{2R'_d} + j\omega x C_2 \frac{3Z_2}{2}} \tag{5}$$

When a line break fault occurs, the three-phase voltages upstream of the fault point are synthesized by the $\dot{U}_{NO}$ and the phase-to-neutral voltages of the voltage source.

$$\begin{cases} \dot{U}_A = \dot{U}_{NO} + \dot{E}_A \\ \dot{U}_B = \dot{U}_{NO} + \dot{E}_B \\ \dot{U}_C = \dot{U}_{NO} + \dot{E}_C \end{cases} \tag{6}$$

The line-to-line voltages at the system side remain symmetrical. For the load side, the line-to-line voltages between the faulty phase and healthy phases change significantly due to the phase-to-earth voltage of the faulty phase. According to (5) and (6), the line-to-line voltages downstream of the fault

point can be written as:

$$\begin{cases} \dot{U}_{A'B} = \dfrac{R'_d \dot{U}_{CB} - 3Z_2 \dot{U}_B}{2R'_d + 3Z_2} \\ \dot{U}_{CA'} = \dfrac{R'_d \dot{U}_{CB} + 3Z_2 \dot{U}_C}{2R'_d + 3Z_2} \\ \dot{U}_{BC} = \sqrt{3}\dot{E}_A \angle -90^\circ \end{cases} \tag{7}$$

C. VOLTAGE CHARACTERISTICS ON BOTH SIDES OF THE FAULT POINT

The existing resonant grounding systems are usually over-compensated. And the detuning factor v is predetermined from -5% to -10% [29]; the normal system damping ratio d of overhead lines is 2% to 5%, and it can increase to 10% when the cover layer breaks [30]. In this paper, we set $v = -10\%$, $d = 10\%$ in the resonant grounding system, and focus on summarizing the steady-state voltage characteristics in small current grounding system under the influence of earthing resistance and fault location.

In the distribution networks with line break fault, O will not change as the base. The voltages at other positions relative to O will change. For the sake of analysis convenience, N is considered to be fixed. Based on fixed N, the trajectory of O relative to N is derived and plotted for different types of line break fault. In the following analysis of voltage magnitudes and phases, $\dot{E}_A$ is taken as the base unit, with its phase set at 0°.

1) SINGLE-PHASE LINE BREAK FAULT WITHOUT EARTHING

According to (1) and (5)-(7), the schematic diagrams of voltages on both sides of the fault point for a single-phase line break without earthing in an ungrounded system and a resonant grounding system are shown in Fig. 2.

Similarity:

The $\dot{U}_{NO}$ is only determined by the location of the fault point. A' is always located at the midpoint of the line segment BC.

For the system side, all line-to-line voltages remain symmetrical, and the sequence of phase-to-earth voltage remains unchanged (A-phase ahead of B-phase, B-phase ahead of C-phase). For the load side, the line-to-line voltage between healthy phases does not change, but the line-to-line voltages between faulty phase and healthy phases decrease to 0.5 times the nominal voltage ($\left|\dot{U}_{BC}\right|/2 = \left|\dot{U}_{A'B}\right| = \left|\dot{U}_{CA'}\right|$). The phases of $\dot{U}_{A'B}$ and $\dot{U}_{CA'}$ are identical; The phases of $\dot{U}_{A'B}$ and $\dot{U}_{CA'}$ are opposite to the phase of $\dot{U}_{BC}$. The sequence of phase-to-earth voltage changes (B-phase ahead of A-phase, C-phase ahead of B-phase).

Difference:

According to Fig. 2, the trajectories of O are different in the two systems. In the ungrounded system, the phase-to-earth voltage magnitude decreases in the healthy phase; the magnitude of phase-to-earth voltage increases/decreases in the faulty phase upstream/downstream of the fault point. On the other hand, in the resonant grounding system, the Petersen coil amplifies the distribution of O. The phase-to-earth voltage of the faulty phase decreases with a small x/k. In extreme cases, where the system only consists of one feeder and the fault point is close to the bus (x/k is large), all phase-to-earth voltages will exceed the nominal voltage as long as there is a sufficiently high earthing resistance.

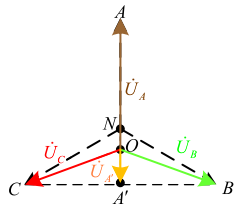

(a) Phase-to-earth voltages in an ungrounded system

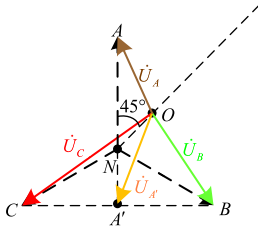

(b) Phase-to-earth voltages in a resonant grounding system

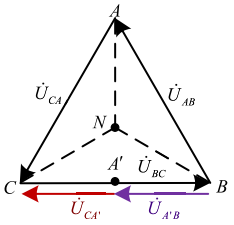

(c) Line-to-line voltages in a small current grounding system

FIGURE 2. Schematic diagrams of voltages on both sides of the fault point for single-phase line break without earthing.

2) SINGLE-PHASE LINE BREAK FAULT WITH EARTHING AT THE SYSTEM SIDE

According to (3) and (5)-(7), the schematic diagrams of voltages on both sides of the fault point for a single-phase line break with earthing at the system side in an ungrounded system and a resonant grounding system are shown in Fig. 3.

Similarity:

The distribution of O is shown in the shaded area in (a) and (b) of Fig. 3. Solely increasing the value of R_d from 0 to ∞ can make O move from A to G along. G denotes the position of O for $R_d = R'_d = \infty$ with different values of x/k. A' is also consistently located at the midpoint of the line segment BC.

The characteristics of line-to-line voltage and the sequence of phase-to-earth voltage are the same as single-phase line break without earthing. When the earthing resistance is small, the characteristics of three phase-to-earth voltages upstream of the fault point are the same as pure single-phase-to-earth fault: the magnitude of phase-to-earth voltage increases/decreases in healthy/faulty phase. The faulty phase-to-earth voltage will be higher than the nominal voltage.

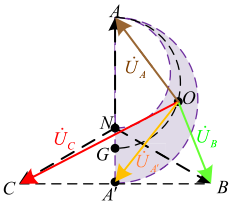

(a) Phase-to-earth voltages in an ungrounded system

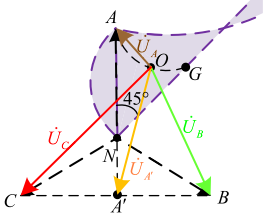

(b) Phase-to-earth voltages in a resonant grounding system

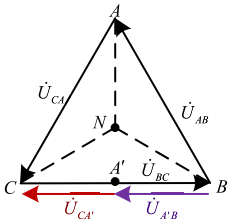

(c) Line-to-line voltages in a small current grounding system

FIGURE 3. Schematic diagrams of voltages on both sides of the fault point for single-phase line break with earthing at the system side.

Difference:

When the earthing resistance is large: in ungrounded systems, the healthy phase-to-earth voltage will decrease, and the magnitude of phase-to-earth voltage will increases/decreases in faulty phase upstream/downstream of the fault point; in resonant grounding systems, the faulty phase-to-earth voltage decreases with a small x/k, but all phase-to-earth voltages will be higher than the nominal voltage with a large x/k.

3) SINGLE-PHASE LINE BREAK FAULT WITH EARTHING AT THE LOAD SIDE

According to (4)-(7), the schematic diagrams of voltages on both sides of the fault point for a single-phase line break with earthing at the load side in an ungrounded system and a resonant grounding system are shown in Fig. 4.

Similarity:

The distribution of O is shown in the shaded area in (a) and (b) of Fig. 4. Increasing only R_d from 0 to ∞ can make O move from A' to G along. Unlike the first two fault types, A' is not consistently positioned at the midpoint of the line segment BC, and its position depends on the load impedance of the faulty feeder and the earthing resistance. According to (5), increasing only R_d will lead to an increase in the magnitude of $\dot{U}_{A'}$, and A will move closer to the midpoint of the line segment BC as well; increasing only Z_2 will result in a decrease in the magnitude of $\dot{U}_{A'}$, and A will move away from the midpoint of the line segment BC.

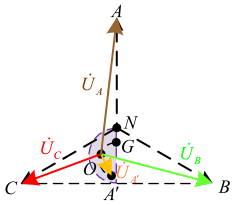

(a) Phase-to-earth voltages in an ungrounded system

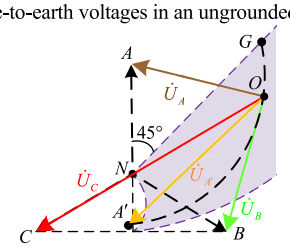

(b) Phase-to-earth voltages in a resonant grounding system

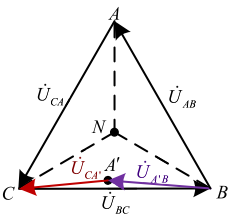

(c) Line-to-line voltages in an ungrounded system

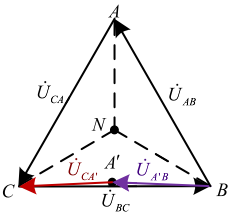

(d) Line-to-line voltages in a resonant grounding system

FIGURE 4. Schematic diagrams of voltages on both sides of the fault point for single-phase line break with earthing at the load side.

The magnitudes summation of the line-to-line voltages between the faulted phase and the healthy phases is 1 to $2/\sqrt{3}$ times the magnitude of the line-to-line voltage between the healthy phases ($|\dot{U}_{BC}| \leq |\dot{U}_{A'B}| + |\dot{U}_{CA'}| < \frac{2}{\sqrt{3}}|\dot{U}_{BC}|$).

Difference:

In ungrounded system, the magnitude of the faulty phase-to-earth voltage upstream of the fault point increases, while the faulty phase-to-earth voltage and at least one healthy phase-to-earth voltage decrease. In a resonant grounding system, when the earthing resistance is small, the magnitude of the faulty phase-to-earth voltage upstream of the fault point increases, while the faulty phase-to-earth voltage and at least one healthy phase-to-earth voltage decrease. However, when the earthing resistance is large and x/k is small, all phase-to-earth voltages will be higher than the nominal voltage.

The range of magnitude and phase of phase-to-earth voltages on both sides of the fault point for single-phase line break faults in small current grounding systems are shown in Table 1.

TABLE 1. The range of magnitude and phase of phase-to-earth voltages on both sides of the fault point for single-phase line break faults in a small current grounding System.

Grounding operation	Earthing side	$\dot{U}_A$		$\dot{U}_B$		$\dot{U}_C$		$\dot{U}_{A'}$	
		Magnitude	Phase	Magnitude	Phase	Magnitude	Phase	Magnitude	Phase
Ungrounded	/	1.00 ~ 1.50	0°	0.87 ~ 1.00	−120° ~ −90°	0.87 ~ 1.00	90° ~ 120°	0 ~ 0.50	−180°
	System	0~1.50	0° ~ 90°	0.40 ~ 1.73	−171.8° ~ −90°	0.87 ~ 1.90	90° ~ 150°	0 ~ 1.50	90° ~ 180°
	Load	1.00~1.50	−12° ~ 0°	0.87~1.15	−120° ~ −90°	0.65~1.00	88° ~ 122°	0~0.50	−90° ~ −180°
Resonant grounding	/	0.57~2.95	0° ~ 120°	0.98 ~ 3.48	150° ~ 180°	1.00~4.51	120° ~ 150°	0.50 ~ 3.93	140° ~ 180°
	System	0 ~ 2.95	−45° ~ 120°	0.97 ~ 3.48	(−180° ~ −120°) ⋃(150° ~ 180°)	0.98~4.51	120° ~ 150°	0.50 ~ 3.93	(−180° ~ −170°) ⋃(120° ~ 180°)
	Load	0.75 ~ 3.19	0° ~ 120°	0.19 ~ 3.48	(−180° ~ −90°) ⋃(133° ~ 180°)	0.97 ~ 4.66	98° ~ 129°	0 ~ 3.93	90° ~ 158°

D. COMPARISON AND SUMMARY OF VOLTAGE CHARACTERISTICS

When a single-phase line break fault occurs in a small current grounding system, the capacitance-to-earth downstream of the fault point is transferred to the healthy phase through the load impedance of the faulty feeder. In addition to the effect of earthing resistance, the imbalance of phase-to-earth admittance in the three phases further contributes to the voltage variation. When comparing the voltage characteristics in an ungrounded system and a resonant grounding system, the summation is shown as follows:

The $\dot{U}_{NO}$ exhibits significant differences between the two systems. The Petersen coil amplifies the distribution of O, and the magnitude of $\dot{U}_{NO}$ in the resonant grounding system can be as high as $1/|v - jd|$ times that of the ungrounded system.

Without considering the damping ratio d, the phase of $\dot{U}_{NO}$ is nearly opposite in the two systems. Line break fault with earthing at one side, increasing only the earthing resistance will cause O move clockwise along a semicircular arc in an ungrounded system. Whereas in a resonant grounding system, O moves counterclockwise along the semicircular arc without considering the d; and moves clockwise along an inferior without considering the d. The angle of the inferior arc is determined by the v and d.

The three-phase voltages upstream of the fault point are synthesized by the $\dot{U}_{NO}$ and the phase-to-neutral voltages of the voltage source. The mathematical expressions for these voltages remain unaffected by the neutral grounding operation. The magnitude of each phase-to-earth voltage in a resonant grounding system is significantly greater than that of an ungrounded system under the same influencing factors, such as the location of the fault point, the ratio of the faulty feeder's capacitance-to-earth to the total system capacitance-to-earth, earthing resistance, and the load impedance.

The similarities of the voltage characteristics in the two systems are as follows. When a line break fault occurs, the faulty phase-to-earth voltage at the load side is synthesized by the other two healthy phase-to-earth voltages and is affected by the earthing resistance of the fault point. It is significantly different from a nominal operation, with a phase angle change exceeding 90°. In the case of ignoring the impedance of distribution line, the healthy phase-to-earth voltage downstream of the fault point matches the healthy phase-to-earth voltage upstream of the fault point. The line-to-line voltages downstream of the fault point between faulty phase and healthy phases experience significant changes due to the influence of the faulty phase-to-earth voltage, and there is a consistent rule: $\left|\dot{U}_{BC}\right| \leq \left|\dot{U}_{A'B}\right| + \left|\dot{U}_{CA'}\right| < \frac{2}{\sqrt{3}}\left|\dot{U}_{BC}\right|$. The sequence of phase-to-earth voltage upstream of the fault point remains unchanged, while the sequence of phase-to-earth voltage downstream of the fault point changes. The voltage change characteristics downstream of the fault point are more obvious than those upstream. Exploiting the voltage information downstream of the fault point allows for local detection of the direction of single-phase line break faults without the need for communication equipment, offering unique advantages.

III. IDENTIFICATION OF LINE BREAK FAULT DIRECTION

A. JUDGING CRITERION

According to the analysis of voltage characteristics for single-phase line break faults in Section I, it is evident that the sequence of phase-to-earth voltage downstream of the fault point changes. Additionally, the magnitude of the line-to-line voltages downstream of the fault point between faulty phase and healthy phases decrease significantly. Based on the above characteristics, a criterion for identifying the direction of single-phase line break faults is designed.

The feeder terminal unit (FTU) on the distribution feeder collects the phase-to-earth voltage data, θ_A, θ_B, θ_C represent the angles of $\dot{U}_A$, $\dot{U}_B$, $\dot{U}_C$, respectively. According to (8), the phase difference between the phase voltages is calculated:

$$\begin{aligned} \theta_{A-B} &= \theta_A - \theta_B \\ \theta_{A-C} &= \theta_A - \theta_C \end{aligned} \tag{8}$$

$\theta_{A-B} > \theta_{A-C}$ represents the sequence of phase-to-earth voltage changes, otherwise the phase sequence remains unchanged. All phase angles and phase differences need to be adjusted to [0, 360°) for calculation.

The FTU collects the line-to-line voltage data. We set p to describe the ratio of the magnitudes of line-to-line voltages.

Set the line-to-line voltage with the largest magnitude to be $\dot{U}_{LMAX}$, and the line-to-line voltage with the lowest magnitude to be $\dot{U}_{LMIN}$. According to (9), the p is calculated:

$$p = \frac{|\dot{U}_{LMAX}|}{|\dot{U}_{LMIN}|} \tag{9}$$

Set U_{set} to the threshold value of "no voltage". To ensure that the line-to-line voltage is not small, the voltage data need to meet (10). In the case of a balanced load, when the system operates normally, $p \approx 1$; when a single-phase line break fault occurs, the line-to-line voltage downstream of the fault point meets the standard of $p > 1$. By setting the threshold value of p, the voltage data that satisfies (10) can provide further indication of single-phase line break faults occurring upstream of the detection point.

$$|\dot{U}_{LMAX}| > U_{set} \tag{10}$$

$$\theta_{A-B} > \theta_{A-C} \tag{11}$$

$$p > p_{set} \tag{12}$$

If the voltage data collected by the FTU meet (10)-(12), it can be judged that a single-phase line break fault has occurred upstream of the detection point. Conversely, it can be judged that no single-phase line break fault occurs upstream of the detection point. The recommended value of U_{set} is 0.2 times the line-to-line voltage rating. When a line break fault occurs, the theoretical minimum value of p is $\sqrt{3}$. Considering the measurement error of the equipment and the imbalanced load situations, initially set $p_{set} = 1.5$. In practical applications, the threshold values mentioned above can be adjusted according to the specific circumstances.

B. FLOWCHART

The flowchart illustrating the process of identifying the direction of single-phase line break faults in small current grounding systems is presented in Fig. 5.

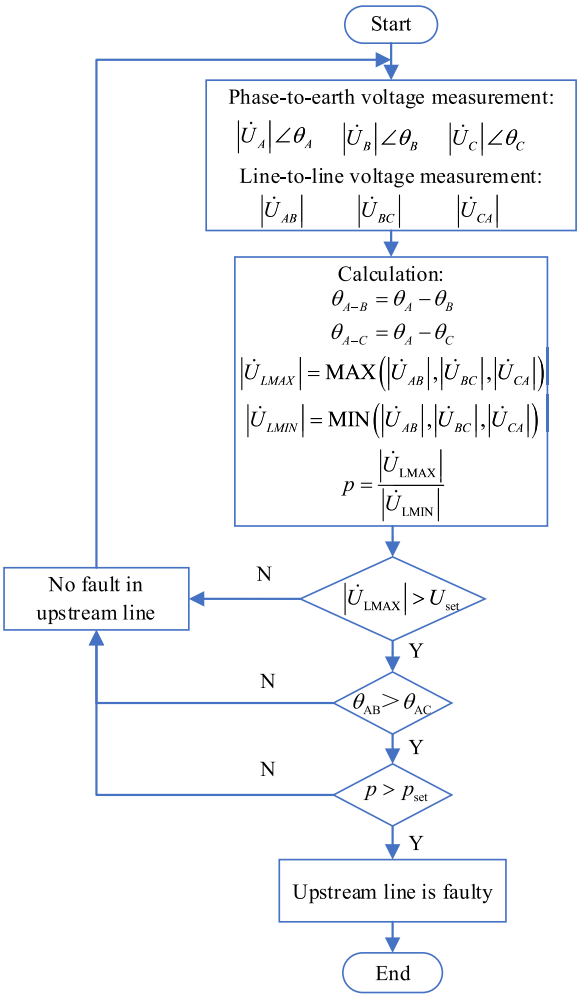

FIGURE 5. Flowchart for identifying the direction of single-phase line break faults in small current grounding systems.

C. INFLUENCING FACTORS AND COUNTERMEASURES

1) V/V WIRED POTENTIAL TRANSFORMER

The capital investment in the distribution network is significantly smaller compared to the transmission network. V/V wired PTs can measure line-to-line voltage with just two single-phase voltage transformers, fulfilling the requirements for measurement and protection. Due to their affordability and minimal space requirements, V/V wired PTs are commonly used in small current grounding systems in suburban and rural areas. However, V/V wired PTs are incapable of measuring phase-to-earth voltage. As a result, the judging criterion should be simplified if the direction of single-phase line break faults needs to be identified in remote areas.

Under the condition that the phase-to-earth voltage cannot be measured, if the voltage data collected by FTU meet (10) and (12), it can be judged that a single-phase line break fault has occurred upstream of the detection point. Conversely, it can be judged that no single-phase line break fault occurs upstream of the detection point. This processing method trades off reliability in fault direction identification for improved adaptability.

2) DISTRIBUTED GENERATION

New energy technology is developing rapidly worldwide, with a significant increase in the connection of DG to the distribution network. According to Section II, a line break fault often leads to voltage changes. The grid-connection regulations of DG require that DG connected to the medium voltage distribution network must possess low voltage ride through (LVRT) capability. Once a voltage drop is detected at the point of common coupling (PCC), the DG enters an LVRT state and outputs three-phase symmetrical positive sequence reactive power to the grid in order to raise PCC voltage.

The assessment criterion of LVRT is shown in Fig. 6. When the PCC voltage is in the area above the voltage contour, the DG should operate continuously without going off-grid; otherwise, the DG is allowed to go off-grid.

The diagram of the relative locations of the PCC and the fault point is shown in Fig. 7. As shown in (a) of Fig. 7,

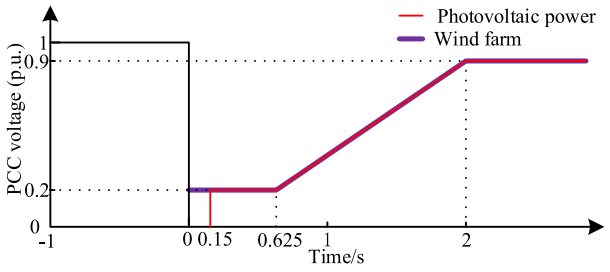

FIGURE 6. The assessment criterion of LVRT.

when the PCC is located upstream of the fault point or on the healthy line, the line break fault characteristics are the same as those of the distribution network without DG. This situation has no effect on the proposed judging criterion.

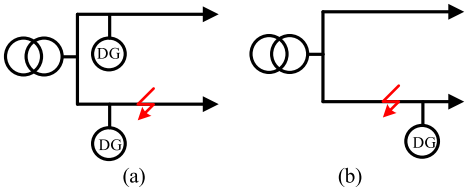

FIGURE 7. The relative locations of the PCC and the fault point.

As shown in (b) of Fig. 7, the PCC is located downstream of the fault point. If the DG can support the downstream load to operate continuously and restore the PCC voltage to a nominal level within a specified time, DG will shift to islanded operation. Conversely, if the DG is unable to support the continuous operation of the downstream load, it will attempt to raise the PCC voltage according to its control strategy during the LVRT state. Eventually, the DG will go off-grid as it fails to comply with the voltage requirements presented in Fig. 6. Once off-grid, the DG has no impact on the fault characteristics of the distribution network. Compared to the distribution network without DG, the process ($\leq$2s) leads to an increase in the line-to-line voltages downstream of the fault point between the faulty phase and healthy phases, and further results in a decrease in p. Furthermore, the sequence of phase-to-earth voltage downstream of the fault point may remain unchanged, reducing the reliability of the proposed judgment criterion. The process is further illustrated by the example of a single-phase line break fault without earthing occurring upstream of the PCC in an ungrounded system.

When a single-phase line break fault occurs, the DG outputs both active and reactive power. Based on Fig. 1 and Fig. 7, the expression of $\dot{U}_{NO}$ can be written as:

$$\dot{U}_{NO} = \frac{x}{2k}\left(\dot{E}_A - \dot{I}_{DGA}Z_2\right) \tag{13}$$

where $\dot{I}_{DGA}$ is the A-phase output current of DG, and its phase angle lags behind the positive sequence voltage of PCC.

According to (13), the phasor diagram of PCC voltage is drawn in Fig. 8.

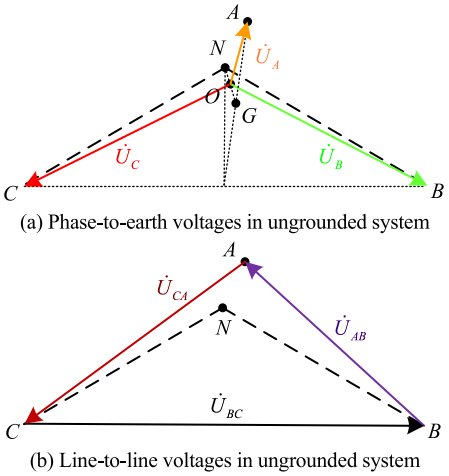

FIGURE 8. Schematic diagram of PCC voltages for a single-phase line break fault without earthing in an ungrounded system.

In this case, the line-to-line voltages downstream of the fault point between the faulty phase and healthy phases increase, while p decreases. In comparison to normal operation, the sequence of phase-to-earth voltage downstream of the fault point remains unchanged. The above results lead to the invalidity of the proposed judging criterion.

Since line break faults do not result in a significant fault current, it is common practice to opt for alarming or delaying the isolation of line break faults, rather than immediately removing the faulty feeder. Therefore, when a line break fault occurs upstream of the PCC, the proposed identification method can reliably detect the direction of the single-phase line break fault only after the DG is off-grid, which does not affect its practicality in the project.

IV. METHOD OF FAULT LOCATION AND PROCESSING

The structure of a typical distribution network is shown in Fig. 9. The FTU on the distribution feeder collects the voltage data and judges whether a single-phase line break fault occurs by using the judging criterion described in Section III. The communication block in Fig. 9 indicates that data can be exchanged between the main station and FTUs with the assistance of communication. The main station collects fault information from each FTU, identifies the fault location based on the fault information, and isolates the faulty feeder for maintenance.

The following illustrates the method of fault location and processing by taking examples of A-phase line break faults occurring at F_1, F_2, and F_3, respectively.

The fault occurs at F_1. When the system cannot communicate, according to the judging criterion, FTU1-2 and FTU5 judge that no single-phase line break fault occurs upstream of the detection point; FTU3-6 judge that a single-phase line break fault occurs upstream of the detection point and issue a warning. When the system can communicate, FTU3-6 further transmit the fault information to the main station through the communications. Then, the main station selects the faulty

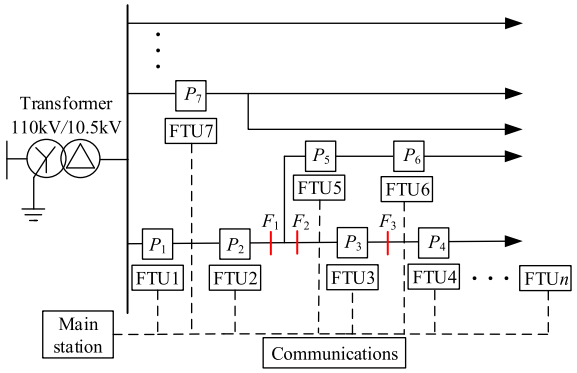

FIGURE 9. Schematic diagram of a typical distribution network.

TABLE 2. Typical parameters of lines.

Type	$R(\Omega/km)$		$L(mH/km)$		$C(\mu F/km)$	
	R_1	R_0	L_1	L_0	C_1	C_0
Cable line	0.080	0.797	0.274	0.956	0.470	0.470
Insulated overhead line	0.270	0.420	1.121	11.513	0.010	0.002
Uncovered overhead line	0.121	0.346	1.019	4.787	0.011	0.004

feeder and traverses the detection points from the system side to the load side of the faulty feeder. If the fault information of adjacent detection points is different, the main station can determine that the fault is located between P_2 and the downstream line branch point, isolate the faulty feeder, and notify the staff to repair.

When a fault occurs at F_2, FTU1-2, FTU5-6, and FTU7 judge that no single-phase line break fault occurs upstream of the detection point, while FTU3-4 judge that a single-phase line break fault occurs upstream of the detection point. Based on the fault information, the main station can locate the fault point between P_3 and the upstream line branch point. When a fault occurs at F_3, FTU1-3, FTU5-6, and FTU7 judge that no single-phase line break fault occurs upstream of the detection point, while FTU4 judges that a single-phase line break fault occurs upstream of the detection point. Based on the fault information, the main station can locate the fault point between P_3 and P_4.

V. CASE STUDY

A. MODEL DESCRIPTION

The simulation model as shown in Fig. 10 is implemented by MATLAB/Simulink. The simulated distribution network consists of a 110kV/10.5kV substation with 7 feeders, including uncovered overhead lines, insulated overhead lines, and cable lines [31]. The typical parameters of the overhead line and cable line are presented in Table 2 [32]. The nominal capacity of the transformer is 20MVA. When the switch S is open, the model is an ungrounded system, and the length of Feeder1 is set to 1km. On the other hand, when the switch S is closed, the model is a resonant grounding system ($v = -10\%$, $d = 10\%$), and the length of Feeder1 is set to 5km. The load

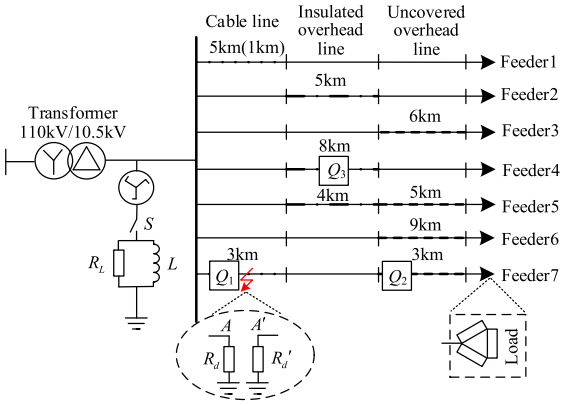

FIGURE 10. Simulation model of single-phase line break faults in a small current grounding system.

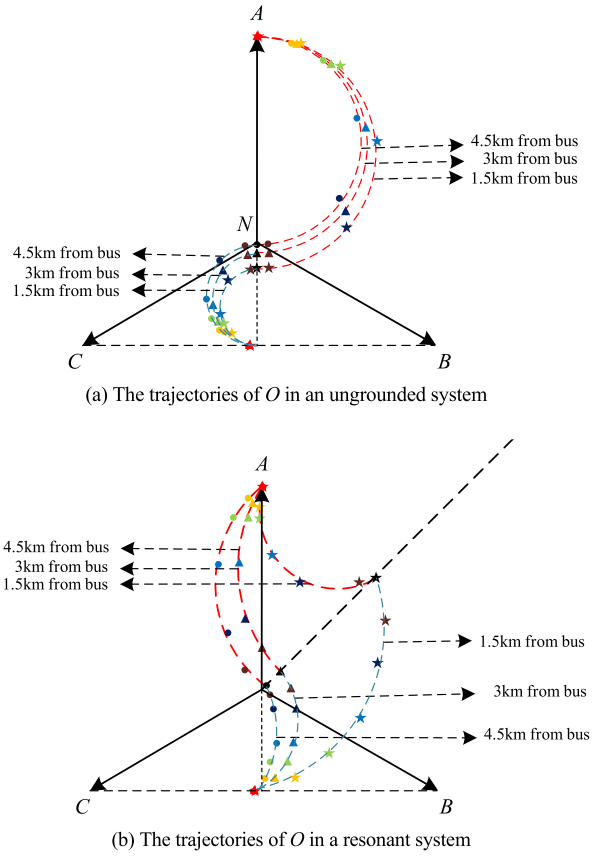

FIGURE 11. The trajectories of O for different fault locations and different earthing resistance.

of each feeder is balanced, and Feeder7 is considered as the faulty feeder, with A-phase as the faulty phase.

Three fault locations are selected: 1.5km, 3km, and 4.5km from the bus. Three types of faults are considered: single-phase line break without earthing, single-phase line break with earthing at the system side, and single-phase line break with earthing at the load side. The earthing resistances are set to 10Ω, 100Ω, 200Ω, 500Ω, 1kΩ, 10kΩ, and ∞.

TABLE 3. Voltages on both sides of the fault point under different fault types.

Fault type	Detection point	$\dot{U}_A$(V)	$\dot{U}_B$(V)	$\dot{U}_C$(V)	$\dot{U}_{AB}$(V)	$\dot{U}_{BC}$(V)	$\dot{U}_{CA}$(V)
Without earthing	Q_1	7042 ∠0.8°	5538 ∠249.7°	5467 ∠110.5°	10410 ∠30.5°	10310 ∠270.0°	10270 ∠150.7°
	Q_2	1919 ∠179.1°	5533 ∠249.4°	5445 ∠110.3°	5207 ∠89.7°	10280 ∠269.7°	5077 ∠89.7°
Earthing at system side	Q_1	4834 ∠47.2°	5946 ∠196.9°	10290 ∠123.5°	10410 ∠30.4°	10310 ∠270.0°	10290 ∠150.7°
	Q_2	6637 ∠147.0°	5966 ∠196.7°	10270 ∠123.4°	5333 ∠88.4°	10280 ∠269.7°	4954 ∠91.1°
Earthing at load side	Q_1	7862 ∠353.5°	6280 ∠259.4°	4296 ∠105.5°	10410 ∠30.5°	10310 ∠270.0°	10270 ∠150.7°
	Q_2	1179 ∠219.9°	6270 ∠259.2°	4276 ∠105.2°	5408 ∠87.1°	10280 ∠269.7°	4888 ∠92.5°

TABLE 4. Voltage data and judgment results of each detection point for single-phase line break faults.

Fault type	Detection point	$\theta_{A\text{-}B}$	$\theta_{A\text{-}C}$	$\theta_{A\text{-}B} > \theta_{A\text{-}C}$	$\lvert\dot{U}_{LMIN}\rvert$(V)	$\lvert\dot{U}_{LMAX}\rvert$(V)	p	$p > p_{set}$	Judgment result	Correctness
Without earthing	Q_1	111.1°	250.3°	×	10270	10410	1.01	×	No fault in upstream line	√
	Q_2	289.7°	68.8°	√	5077	10280	2.02	√	Upstream line is faulty	√
	Q_3	111.1°	250.5°	×	10160	10290	1.01	×	No fault in upstream line	√
Earthing at system side	Q_1	210.3°	283.7	×	10290	10410	1.01	×	No fault in upstream line	√
	Q_2	310.3°	23.6°	√	4954	10280	2.08	√	Upstream line is faulty	√
	Q_3	211.2°	284.0°	×	10180	10300	1.01	×	No fault in upstream line	√
Earthing at load side	Q_1	94.1°	248.0°	×	10270	10410	1.01	×	No fault in upstream line	√
	Q_2	320.7°	114.7°	√	4888	10280	2.10	√	Upstream line is faulty	√
	Q_3	93.9°	248.7°	×	10160	10290	1.01	×	No fault in upstream line	√

Three detection points are set: Q_1 and Q_2 on Feeder7, which are 1 km and 4 km away from the bus respectively, and Q_3 on Feeder4, which is 4km away from the bus.

B. SIMULATION OF FAULT CHARACTERISTIC

The trajectories of O for different fault locations and different earthing resistances are shown in Fig. 11.

For different types of single-phase line break faults in an ungrounded system, the earthing resistance of 500Ω and the fault location of 1.5km from the bus are taken as examples. The voltages measured by the detection points (Q_1 and Q_2) on both sides of the fault point are shown in Table 3.

According to Table 3, the faulty phase-to-earth voltage downstream of the fault point is significantly different from the nominal operation, with a phase angle change greater than 90°. The sequence of the phase-to-earth voltage upstream of the fault point remains unchanged, while the sequence of the phase-to-earth voltage downstream of the fault point changes. The line-to-line voltages upstream of the fault point remain symmetrical. However, the line-to-line voltages downstream of the fault point between the faulty phase and the healthy phases change significantly, decreasing to 0.5 times the nominal voltage. The phases of $\dot{U}_{A'B}$ and $\dot{U}_{CA'}$ are nearly identical, while the phases of $\dot{U}_{A'B}$ and $\dot{U}_{CA'}$ are nearly opposite to the phase of $\dot{U}_{BC}$.

C. SIMULATION OF FAULT DIRECTION IDENTIFICATION

The voltage data in Table 3 is further analyzed to verify the correctness of the proposed fault direction method. According to A of Section I, the threshold value of "no voltage" is set at 2100V ($U_{set} = 2100$V); the threshold value of p is set at 1.5 ($p_{set} = 1.5$). The voltage data collected at each detection point and the judgment results are shown in Table 4.

According to Table 4, the FTU is capable of determining the occurrence of single-phase line break faults and indicating the fault direction based on the criteria proposed in this paper. The judgment results of each detection point are accurate. Using the fault location method described in Section IV, the fault can be narrowed down to a region between Q_1 and Q_2.

In order to test the performance of the proposed method, numerous simulation experiments were conducted by varying the grounding operation, feeder length, fault location, earthing resistance, and load impedance. Due to limitations in the length of this paper, the remaining data from these experiments are not presented. All the simulation results confirm that the described fault characteristics are correct and that the fault direction identification method effectively indicates the fault direction.

VI. CONCLUSION

This paper proposes a method for identifying the direction of single-phase line break faults in small current grounding systems by utilizing the local voltage change characteristics. Theoretical analysis and simulations lead to the following conclusions:

1) The line-to-line voltages upstream of the fault point remain symmetrical. However, the line-to-line voltages downstream of the fault point, between the faulty phase and the healthy phases, decrease to 0.5 times the nominal voltage. Additionally, their phases are either approximately the same or approximately opposite.
2) The faulty phase downstream of the fault point experiences an angle change greater than 90°. The sequence of phase-to-earth voltage upstream of the fault point remains unchanged, but the sequence of phase-to-earth voltage downstream of the fault point does change.
3) The variation range of phase-to-earth voltages during a single-phase line break fault is greater in a resonant grounding system compared to an ungrounded system, leading to potentially severe damage to the network insulation. The maximum phase-to-earth voltage can reach up to $4.66\left|\dot{E}_A\right|$ in resonant grounding systems and $1.90\left|\dot{E}_A\right|$ in ungrounded systems.
4) The fault direction identification method is based on the voltage change information downstream of the fault point. It considers both the magnitude of the line-to-line voltage and the sequence of phase-to-earth voltage. Therefore, this method is more reliable compared to that relying solely on single fault information.
5) The proposed method can use the existing equipment in distribution networks to indicate the fault direction and further locate the fault point with the assistance of communication. Therefore, there is no need for any additional investment to implement this identification method.
6) The fault direction identification method is not influenced by earthing resistance and load impedance, and can adapt to the high utilization rate of V/V wired PT in the distribution network. The connection of DGs to the distribution network will not affect the feasibility of this method in the project.

This paper systematically studies the voltage characteristics of single-phase line break faults in small current grounding systems. It provides theoretical support for future research on detection and location approaches. The proposed identification method offers a reliable way to determine the direction of single-phase line break faults, thereby improving the level of relay protection in distribution networks in future practical applications.

However, it should be noted that the fault direction identification method proposed in this paper is unable to directly trip the circuit breaker using the information upstream of the fault point. In future studies, it is necessary to explore fault identification methods for line break faults that utilize the upstream fault information to enable direct cooperation with the circuit breaker. This would facilitate the swift disconnection of the downstream fault line and effectively isolate the fault. In addition, this paper does not consider multiphase line break faults. Although multiphase line break faults occur relatively infrequently, it is imperative to investigate them in order to enhance the theoretical understanding of line break faults.

REFERENCES

[1] L. Guo, Y. Xue, and B. Xu, "Research on effects of neutral grounding modes on power supply reliability in distribution networks," *Power Syst. Technol.*, vol. 39, pp. 2340–2345, 2015.
[2] R. Burgess and A. Ahfock, "Minimising the risk of cross-country faults in systems using arc suppression coils," *IET Gener., Transmiss. Distrib.*, vol. 5, no. 7, pp. 703–711, 2011.
[3] Z. Fu, N. Wang, L. Huang, and R. Zhang, "Study on neutral point grounding modes in medium-voltage distribution network," in *Proc. Int. Symp. Comput., Consum. Control*, Jun. 2014, pp. 154–157.
[4] B. Xu, Y. Xue, and G. Feng, "Discussion on several problems of earthing fault protection in distribution network," *Autom. Electric Power Syst.*, vol. 43, no. 20, pp. 1–7, 2019.
[5] P. Wang, B. Chen, C. Tian, B. Sun, M. Zhou, and J. Yuan, "A novel neutral electromagnetic hybrid flexible grounding method in distribution networks," *IEEE Trans. Power Del.*, vol. 32, no. 3, pp. 1350–1358, Jun. 2017.
[6] A. M. Ershov, A. V. Khlopova, and A. I. Sidorov, "Technological violations on overhead lines with voltage of 10 kv," in *Proc. Int. Conf. Ind. Eng., Appl. Manuf. (ICIEAM)*, May 2020, pp. 1–5.
[7] S. Prakash and S. Mishra, "VSC control of grid connected PV for maintaining power supply during open phase condition in distribution network," in *Proc. IEEMA Engineer Infinite Conf. (eTechNxT)*, Mar. 2018, pp. 1–6.
[8] A. N. Klochkov, "The device for the detection of three-phase networks with phase wire breakage," *Bull. KrasGAU*, vol. 3, no. 1, pp. 221–223, 2011.
[9] R. M. Sherstobitov and M. A. Yundin, "Reliability indicators of a 10kV OHL network," *Agricult. Mechanization Electrific.*, vol. 6, no. 1, pp. 17–18, 2011.
[10] W. Tao, Y. Tiejun, W. Wenzhen, J. Peng, G. Jieting, and L. Kai, "Research on key technologies of thunder detection in zibo distribution network," in *Proc. 2nd IEEE Conf. Energy Internet Energy Syst. Integr. (EI2)*, Oct. 2018, pp. 1–6.
[11] L. Qin, L. Zhang, P. Wang, and F. Shi, "Single-phase disconnection fault location method based on negative sequence current distribution feature," in *Proc. IEEE 4th Int. Electr. Energy Conf. (CIEEC)*, May 2021, pp. 1–5.
[12] L. Zichang, L. Yadong, Y. Yingjie, W. Peng, and J. Xiuchen, "An identification method for asymmetric faults with line breaks based on low-voltage side data in distribution networks," *IEEE Trans. Power Del.*, vol. 36, no. 6, pp. 3629–3639, Dec. 2021.
[13] R. A. Wilson and V. Vadlamani, "Detecting open phase conductors," in *Proc. 68th Annu. Conf. Protective Relay Eng.*, College Station, TX, USA, 2015, pp. 319–324.
[14] S. Yu and L. Pan, "Analysis of not-short circuit faults in neutral indirectly grounding system," *Power Syst. Protection Control*, vol. 37, no. 20, pp. 74–78, 2009.
[15] Z. Chang, G. Song, and X. Wang, "Fault identification and isolation of distribution network based on zero-sequence voltage amplitude difference," *Autom. Electric Power Syst.*, vol. 42, no. 6, pp. 135–139, 2018.

[16] P. Lu, W. Wang, Q. Yu, B. Fan, P. Liu, F. Wang, and X. Zeng, "Permanent single-line-to-ground fault removal method for ferro-resonance avoidance in neutral ungrounded distribution network," *IEEE Access*, vol. 10, pp. 53724–53734, 2022.
[17] L. Niu, G. Wu, and Z. Xu, "Single-phase fault line selection in distribution network based on signal injection method," *IEEE Access*, vol. 9, pp. 21567–21578, 2021.
[18] X. Wei, X. Wang, J. Gao, D. Yang, K. Wei, and L. Guo, "Faulty feeder detection for single-phase-to-ground fault in distribution networks based on transient energy and cosine similarity," *IEEE Trans. Power Del.*, vol. 37, no. 5, pp. 3968–3979, Oct. 2022.
[19] B. Olejnik, "Adaptive zero-sequence overcurrent criterion for Earth fault detection for fault current passage indicators in resistor grounded medium voltage networks," *IEEE Access*, vol. 9, pp. 63952–63965, 2021.
[20] A. Kalyuzhny, "Analysis of temporary overvoltages during open-phase faults in distribution networks with resonant grounding," *IEEE Trans. Power Del.*, vol. 30, no. 1, pp. 420–427, Feb. 2015.
[21] Y. Xue, M. Chen, and L. Cao, "Analysis of voltage characteristics of single-phase disconnection fault in ungrounded distribution system," *Proc. Chin. Soc. Electr. Eng.*, vol. 41, no. 4, pp. 1322–1333, 2021.
[22] H. Li, Y. Xue, M. Chen, and Z. Zhang, "Analysis of voltage characteristics for single-phase line break fault in resonant grounding systems," *IEEE Trans. Power Del.*, vol. 38, no. 2, pp. 1416–1425, Apr. 2023.
[23] A. C. Adewole, A. Rajapakse, D. Ouellette, and P. Forsyth, "Residual current-based method for open phase detection in radial and multi-source power systems," *Int. J. Electr. Power Energy Syst.*, vol. 117, May 2020, Art. no. 105610.
[24] Q. Kang, W. Cong, M. Wang, G. Xian, G. Liu, Z. Guo, and R. Yi, "Analyses and judgment methods of single-phase broken-line fault for loaded distribution line," in *Proc. IEEE PES Asia–Pacific Power Energy Eng. Conf. (APPEEC)*, Oct. 2016, pp. 482–486.
[25] Y. Wu, X. Meng, and S. Guan, "Optimized deep learning based single-phase broken fault type identification for active distribution networks," in *Proc. 3rd Int. Conf. Power Eng.*, vol. 9, 2023, pp. 119–126.
[26] J. Liu, Y. Zhou, Y. Li, G. Lin, W. Zu, Y. Cao, X. Qiao, C. Sun, Y. Cao, and C. Rehtanz, "Modelling and analysis of radial distribution network with high penetration of renewable energy considering the time series characteristics," *IET Gener., Transmiss. Distribution*, vol. 14, no. 14, pp. 2800–2809, Jul. 2020.
[27] Y. Zhang, J. Suo, and B Xu, "Detection of PT breaking based on the theory of line voltage amplitude comparison," *Relay*, vol. 12, pp. 6–22, Jan. 2005.
[28] *IEEE Guide for the Parameter Measurement of AC Transmission Lines*, IEEE Standard 1870-2019, 2019.
[29] Z. Chen, W. Wu, J. Chen, and Q. Zhang, "Discussion on damp rate and out-of-resonance degree of power compensation network," *Relay*, vol. 33, pp. 36–39, Feb. 2005.
[30] Y. Zhang, Q. Chen, and L. Cheng, "Novel method for measuring capacitive current and distinguishing high-resistance grounding of distributing network," *Automat. Electric Power Syst.*, vol. 32, pp. 83–101, Mar. 2008.
[31] Z. Chang, G. Song, and W. Zhang, "Characteristic analysis and fault segment location on negative sequence voltage and current of single phase line breakage fault in distribution network," *Power Syst. Technol.*, vol. 44, no. 8, pp. 3065–3074, 2020.
[32] D. Xue, G. Li, and B. Xu, "Measuring method of capacitance to ground in resonant grounding system based on transient information after arc extinguishing," *Trans. China Electrotechnical Soc.*, vol. 35, no. 7, pp. 1521–1528, 2020.

FAN YANG was born in 1982. He received the Ph.D. degree in electrical engineering from Wuhan University, Wuhan, China, in 2011. He is currently a professor-level Senior Engineer with the Electric Power Research Institute, State Grid Hubei Electric Power Company. His current research interests include active distribution network protection technology, distributed power generation, and micro grid integration technology.

HE LI was born in 1999. He received the bachelor's degree in electrical engineering and automation from the China University of Petroleum (East China), Qingdao, China, in 2021, where he is currently pursuing the master's degree in electrical engineering. His research interest includes single-phase line break fault detection.

WEI HU was born in 1981. She received the B.S.E.E. degree in power system and its automation from North China Electric Power University, Beijing, China, in 2004, and the Ph.D. degree in power electronics and power transmission from Wuhan University, Wuhan, China, in 2015. She is currently a Senior Engineer with the Electric Power Research Institute, State Grid Hubei Electric Power Company. Her current research interests include distribution network planning and operation analysis.

YANG LEI was born in 1988. He received the master's degree in power system and its automation from Wuhan University, Wuhan, China, in 2013. He is currently a Senior Engineer with the Electric Power Research Institute, State Grid Hubei Electric Power Company. His current research interests include power system relay protection and distribution automation.

HECHONG CHEN was born in 1994. He received the Ph.D. degree in electrical engineering from Wuhan University, Wuhan, China, in 2022. He is currently an Engineer with the Electric Power Research Institute, State Grid Hubei Electric Power Company. His current research interests include active distribution network protection technology, distributed power generation, and micro grid integration technology.

YONGDUAN XUE (Member, IEEE) received the B.S., M.S., and Ph.D. degrees from Xi'an Jiaotong University, Xi'an, China, in 1992, 1997, and 2003, respectively. He is currently a Professor with the College of New Energy, China University of Petroleum (East China), Qingdao, China. His research interests include grounding fault self-healing technology, electric shock, and electrical fire safety protection.